An Experimental Study of the Gas-Phase Reactions of NO3 Radicals with a Series of Unsaturated Aldehydes: trans-2-Hexenal, trans-2-Heptenal, and trans-2-Octenal

5 AUTHORS, INCLUDING:

Jean-Francois Doussin

Université Paris-Est Créteil Val de Marne - Univ…

**107** PUBLICATIONS **845** CITATIONS

SEE PROFILE

An Experimental Study of the Gas-Phase Reactions of NO₃ Radicals with a Series of Unsaturated Aldehydes: *trans*-2-Hexenal, *trans*-2-Heptenal, and *trans*-2-Octenal

Jamila Kerdouci, Bénédicte Picquet-Varrault,* Régine Durand-Jolibois, Cécile Gaimoz, and Jean-François Doussin

Laboratoire Interuniversitaire des Systèmes Atmosphériques, UMR CNRS 7583, Université Paris Est Créteil (UPEC) et Université Paris Diderot (UPD), Institut Pierre Simon Laplace, 61 Avenue du Général de Gaulle, 94010 cedex Créteil, France

S *Supporting Information*

ABSTRACT: Rate constants for the gas-phase reactions of the NO₃ radical with a series of unsaturated aldehydes, *trans*-2-hexenal, *trans*-2-heptenal, and *trans*-2-octenal, have been measured using absolute rate method at 294 ± 3 K and atmospheric pressure. This work was performed to clarify discrepancies found in the literature and thus led to a clearer view of the effect of the increasing carbon chain length on the reactivity of *trans*-2-alkenals. The rate constants were determined to be $(4.7 \pm 1.5) \times 10^{-15}$, $(5.3 \pm 1.6) \times 10^{-15}$, and $(5.6 \pm 2.3) \times 10^{-15}$ cm³ molecule⁻¹ s⁻¹ for *trans*-2-hexenal, *trans*-2-heptenal, and *trans*-2-octenal, respectively. These results clearly indicate that the carbon chain lengthening of the *trans*-2-alkenals does not significantly affect the rate constant. In addition, the mechanism for the reaction of NO₃ with these unsaturated aldehydes was also investigated. Unsaturated peroxynitrate-type compounds that are exclusively formed through the abstraction channel were observed as the main products.
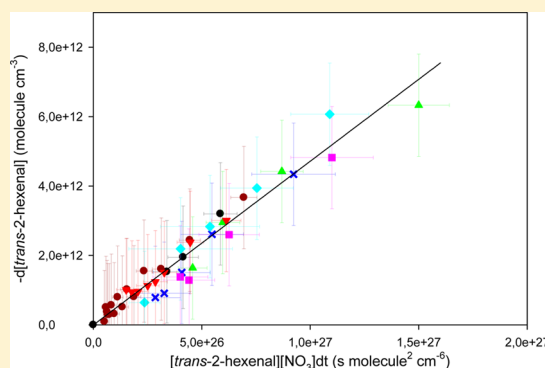
INTRODUCTION

Carbonyl compounds are emitted into the atmosphere from anthropogenic and biogenic sources. They are emitted by the incomplete combustion of fuels.[1−4] Moreover, in addition to the emissions of isoprene and terpenes, a large variety of oxygenated compounds have been observed as plant emissions.[5,6] This is in particular the case of C6 oxygenates,[7−9] such as *trans*-2-hexenal (also called leaf aldehyde), which are emitted from wounded leaves. Other aldehydes such as *trans*-2-heptenal and *trans*-2-octenal have also been identified in the emissions of plants.[10−13] Besides these primary sources, carbonyl compounds are also formed in the atmosphere from the photo-oxidation of organic compounds. The oxidation of terpenes and conjugated dienes produces a number of unsaturated carbonyl compounds.[14−16] For these reasons, unsaturated aldehydes play a key role in the tropospheric chemistry as a source of HO$_x$ radicals and as possible intermediates in the formation of secondary organic aerosols.[17,18]

These unsaturated aldehydes are mainly removed from the atmosphere by photolysis and by the gas-phase reaction with OH and NO₃ radicals and O₃.[16,17,19] Ozone and NO₃ radical are known to be the main oxidants of VOC during the night.[20,21] In particular, NO₃ oxidation of unsaturated VOC, which proceeds mainly by an electrophilic addition on the double bond, is often a fast reaction. Consequently, oxidation by NO₃ is expected to be a significant loss process of

unsaturated aldehydes. Several kinetic studies have been carried out for the reactions of C4−C7 *trans*-2-alkenals with nitrate radicals[22−26] and are reported in Figure 1. One can observe that
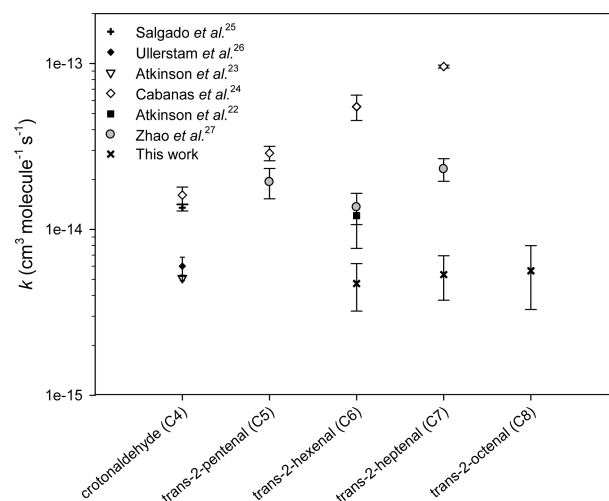

Figure 1. Rate constants for gas-phase reactions of NO₃ radical with a series of *trans*-2-alkenals (in logarithmic scale).
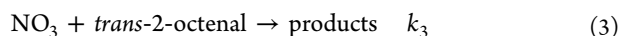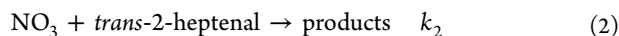
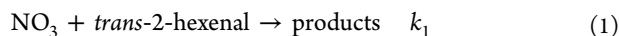there are very large discrepancies between published data. Indeed, the values reported by Cabañas et al.[24] reveal a strong increase in the rate constant with increasing alkyl chain length, whereas the values published by Atkinson et al.[22] and more recently by Zhao et al.[27] do not confirm this large increase in the rate constants.

Thus in this work, we have performed kinetic and mechanistic studies for the gas-phase reactions of NO_3 radicals with trans-2-hexenal (trans-$CH_3(CH_2)_2CH$=$CHCH(O)$), trans-2-heptenal (trans-$CH_3(CH_2)_3CH$=$CHCH(O)$), and trans-2-octenal (trans-$CH_3(CH_2)_4CH$=$CHCH(O)$)

$$NO_3 + \text{trans-2-hexenal} \rightarrow \text{products} \quad k_1 \tag{1}$$

$$NO_3 + \text{trans-2-heptenal} \rightarrow \text{products} \quad k_2 \tag{2}$$

$$NO_3 + \text{trans-2-octenal} \rightarrow \text{products} \quad k_3 \tag{3}$$

The aim was here to determine the effect of the alkyl chain length on the reactivity of the trans-2-alkenals. This study on a series of unsaturated aldehydes is also essential for the development of reliable structure activity relationships (SAR) for this class of compounds. In particular, it will be used to complete the SAR which was developed recently in our group.[28]

■ EXPERIMENTAL SETUP AND PROCEDURES

Experiments were carried out in an evacuable chamber, consisting of a Pyrex reactor of 977 L coupled to two multiple reflection optical systems interfaced to a FTIR spectrometer and a UV−visible grating spectrometer. The main features of this chamber and its spectroscopic devices have previously been described;[29,30] thus only the relevant details are given here. The quantification of the organic compounds in the reactor was performed by using FTIR spectroscopy. The FTIR spectrometer is a BOMEM DA8-ME equipped with a glowbar as mid-infrared source. Infrared spectra were acquired by averaging 100 scans at a resolution of 0.5 cm^{-1} and with an optical path length of 204 m. For absolute rate determination, NO_3 was monitored by its visible absorption at 662 nm using UV−visible spectrometry. This spectrometer consists of a source (high-pressure xenon arc lamp, Osram XBO, 450WXe UV), a multipass optical system inside the reactor (path length of 72 m), a monochromator (HR 320 Jobin-Yvon), and a 1024 × 58 pixel charge-coupled device (CCD) camera (CCD 3000, Jobin-Yvon) as a detector. In this configuration, the CCD covers a spectral range of ca. 60 nm, and the instrument has a maximum resolution of 0.15 nm.

NO_3 radicals were generated by thermal decomposition of N_2O_5,[31] which was synthesized in a vacuum line by the reaction of NO_2 with excess of O_3 according to reaction 4 and followed by reaction 5

$$NO_2 + O_3 \rightarrow NO_3 + O_2 \tag{4}$$

$$NO_3 + NO_2 \leftrightarrow N_2O_5 \tag{5}$$

In the first stage of the synthesis, NO_2 was trapped at 193 K in a cold tube. Ozone was then flushed onto the NO_2 crystals, whereas the cold trap was moved to a second tube where formed dinitrogen pentoxide crystals were collected. At the end of the synthesis, the bulb containing dinitrogen pentoxide crystals was evacuated down to remove remaining NO_2 at room temperature. N_2O_5 was hence purified by trap-to-trap distillation and could be kept for several weeks in the cold trap under vacuum.

All experiments were performed in the dark at 294 ± 3 K and at atmospheric pressure with synthetic air (80% N_2 + 20% O_2). In a first step, the trans-2-alkenal was injected into the chamber, and its concentration was measured for approximately one hour to check for adsorption on the chamber walls. Initial concentrations of trans-2-alkenals were (3.3−8.4) × 10^{13} molecules cm^{-3}. Then, N_2O_5 was introduced by stepwise injections in order to ensure measurable consumption of the VOC on a reasonable time scale. For each experiment, a total, of two to three additions of N_2O_5 were performed (each addition corresponding to an initial concentration of NO_3 in the chamber of approximately (3−40) × 10^{10} molecules cm^{-3}). The mixing of N_2O_5 in the reactor is ensured by a mixing pipe (a pyrex line equipped with many small radial holes which is installed all across the simulation chamber). N_2O_5 is introduced and flushed with N_2 as carrier gas into the line that allows introducing it in the whole length of the reactor. The efficiency of this mixing system has been checked in the past and allows a good mixing at the few seconds' scale which is very fast in comparison to the duration of visible and infrared spectra (respectively 1 min and 3−4 min). During the course of the experiment, time-resolved concentrations of organic reactants and products were monitored from their infrared spectral absorptions. Integrated band intensities (IBIs) used to quantify these species are: IBI$_{\text{trans-2-hexenal}}$ (1190−1115 cm^{-1}) = (2.6 ± 0.3) × 10^{-18} cm/molecule, IBI$_{\text{trans-2-heptenal}}$ (1015−945 cm^{-1}) = (2.4 ± 0.1) × 10^{-18} cm/molecule, and IBI$_{\text{trans-2-octenal}}$ (1025−930 cm^{-1}) = (3.6 ± 0.9) × 10^{-18} cm/molecule (base e). NO_3 was monitored from its visible absorption using the cross section of its main absorption band at 662 nm equal to 2.1 × 10^{-17} cm^2/molecule (base e) which is the value recommended by IUPAC.[32] UV−visible spectra were treated using DOASIS software developed by IUP Heidelberg group (https://doasis.iup.uni-heidelberg.de/bugtracker/projects/doasis/)). Figure S1 of the Supporting Information shows a typical plot of an experiment where concentrations of reactants (trans-2-hexenal and NO_3), products (peroxynitrate (PAN) analogues and CO), and NO_2 were monitored by IR and UV−visible spectrometric devices. Unfortunately, due to a saturation of its absorption bands, N_2O_5 could not be monitored during the experiments.

The sources of chemicals used and their purities were: trans-2-hexenal (>99%) from Acros Organics; trans-2-heptenal (>97%) from Sigma-Aldrich; trans-2-octenal (>94%) from Sigma-Aldrich. Dry synthetic air was generated using N_2 (from liquid nitrogen evaporation, purity >99.995%, H_2O < 5 ppm, MESSER) and O_2 (Alphagaz 1, purity > 99.995%, H_2O < 3 ppm, C_nH_m < 0.5 ppm, Air Liquide).

■ RESULTS AND DISCUSSION

Kinetic Study. A minimum of three experiments were performed for each aldehyde. The NO_3 oxidation rate constants were obtained by using the absolute rate technique. If it is assumed that the loss of the trans-2-alkenal is due solely to the reaction 6 with nitrate radicals

$$\text{trans-2-alkenal} + NO_3 \rightarrow \text{products} \tag{6}$$
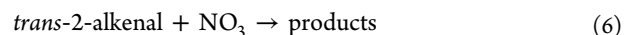
the second-order kinetic equation for reaction 6 is

$$\frac{-[\text{trans-2-alkenal}]}{dt} = k_6[\text{trans-2-alkenal}][NO_3] \tag{I}$$

This equation can be approximated for small time intervals

$$-\Delta[\textit{trans}\text{-2-alkenal}] = k_6[\textit{trans}\text{-2-alkenal}][NO_3]\Delta t \qquad (II)$$

Where $-\Delta[\textit{trans}\text{-2-alkenal}]$ corresponds to the consumption of $\textit{trans}$-2-alkenal during the time interval Δt and [$\textit{trans}$-2-alkenal] and $[NO_3]$ are averaged concentrations during this interval. By plotting $-\Delta[\textit{trans}\text{-2-alkenal}]$ vs [$\textit{trans}$-2-alkenal] $\times$ $[NO_3] \times \Delta t$, a straight line with a slope corresponding to k_6 is obtained. Data from all experiments are exhibited in Figures 2−4 for $\textit{trans}$-2-hexenal, $\textit{trans}$-2-heptenal, and $\textit{trans}$-2-octenal,

Figure 2. Absolute rate plot for the gas-phase reaction of $\textit{trans}$-2-hexenal with NO_3 radicals. Different symbols indicate independent experiments.

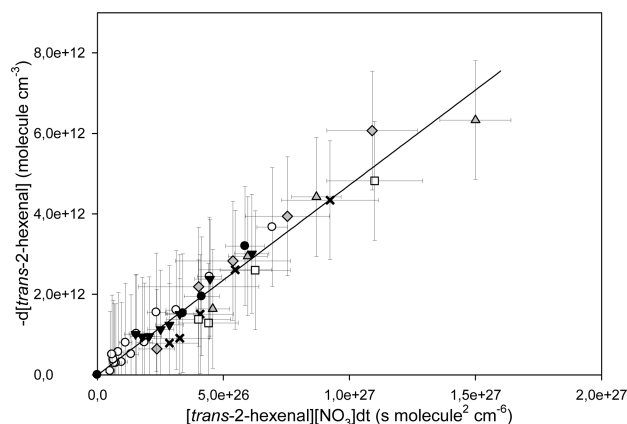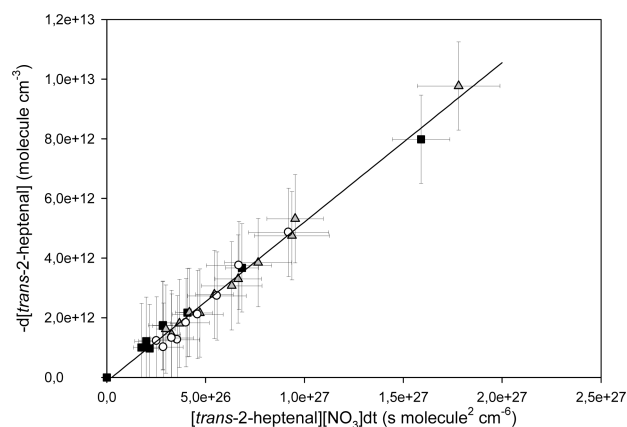**Figure 3.** Absolute rate plot for the gas-phase reaction of $\textit{trans}$-2-heptenal with NO_3 radicals. Different symbols indicate independent experiments.

respectively. It can be observed that all individual experiments are in good agreement. As a consequence, all data points were combined, and a linear regression, which takes into account errors on both abscissa and ordinate scales, was performed using the program developed by Brauers and Finlayson-Pitts.[33] The errors on both abscissa and ordinate scales were estimated from the error on NO_3 and $\textit{trans}$-2-alkenal concentrations, which were taken as 7×10^9 and 7.38×10^{11} molecules cm^{-3}, respectively. These errors correspond to the uncertainty on the estimation of band intensities in visible and infrared spectra. The uncertainties on NO_3 cross sections and on Δt were considered to be negligible here and thus were not taken into account. The quoted uncertainties on the rate constants are the 2σ, where σ is the standard deviation on the linear regression.
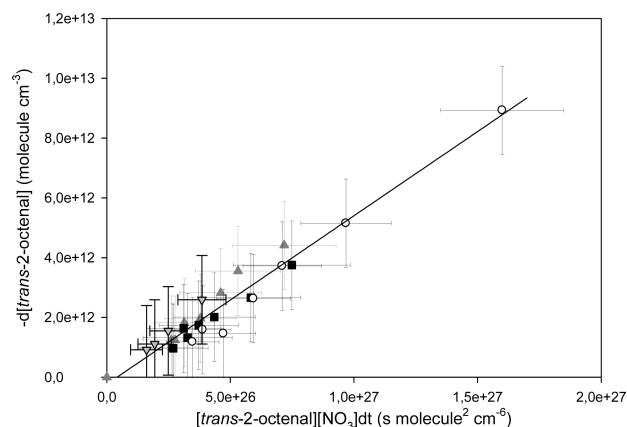

Figure 4. Absolute rate plot for the gas-phase reaction of $\textit{trans}$-2-octenal with NO_3 radicals. Different symbols indicate independent experiments.

Table 1. Rate Constants for the Oxidation of a Series of Unsaturated Aldehydes by the NO_3 Radical

compound	$k_{NO_3} \times 10^{14}$ (cm^3 molecule^{-1} s^{-1})	method	ref
$\textit{trans}$-2-hexenal	1.36 ± 0.29	relative rate	Zhao et al.[27]
	5.49 ± 0.95	absolute rate	Cabañas et al.[24]
	1.21 ± 0.44	relative rate	Atkinson et al.[22]
	0.47 ± 0.15	**absolute rate**	**this work**
$\textit{trans}$-2-heptenal	2.31 ± 0.36	relative rate	Zhao et al.[27]
	9.59 ± 0.19	absolute rate	Cabañas et al.[24]
	0.53 ± 0.16	**absolute rate**	**this work**
$\textit{trans}$-2-octenal	**0.56 ± 0.23**	**absolute rate**	**this work**

Table 1 summarizes the rate constants measured by this work with data from literature for the reactions of the NO_3 radical with the series of $\textit{trans}$-2-alkenals. The rate constant for $\textit{trans}$-2-hexenal has already been measured by three studies. Two of them are relative rate studies (Atkinson et al.[22] and Zhao et al.[27]). The third one is an absolute determination in a fast-flow discharge system using laser-induced fluorescence (LIF) for the NO_3 radical detection (Cabañas et al.[24]). Concerning the $\textit{trans}$-2-heptenal, two values have been published by Cabañas et al.[24] and Zhao et al.[27] For $\textit{trans}$-2-octenal, this work provides the first experimental determination.

Our k_1 value differs significantly from those obtained by the previous determinations by factors from 3 to 12. Similarly, our k_2 value obtained for $\textit{trans}$-2-heptenal is also much lower than those measured by Zhao et al.[27] and Cabañas et al.[24] by factors of 4 and 18, respectively.

Moreover, it can be noticed that the rate constants reported by Cabañas et al.[24] are systematically higher than the other determinations. In their experiments, the rate constants were determined by monitoring the decay of NO_3 radical and $\textit{trans}$-2-alkenals in a flow-tube system. However the studies of Ullerstam et al.[34] and D'anna et al.[35] on the reactivity of saturated aldehydes have shown that secondary reactions of NO_3 radicals with RCO radicals (produced after H-atom abstraction from the −CHO groups) occurs with this type of experimental devices and thus may lead to higher rate

constants. Moreover as suggested by Zhao et al.,[27] heterogeneous wall reactions involving the VOC might have occurred. In our experiments, rate constants were determined by monitoring the decay of the VOC, which may be less subject to secondary reactions than the NO_3 radical (which reacts with many other species in the mixture). In addition, it was checked that aldehydes were stable in the chamber in absence of NO_3 radicals. These hypotheses may explain the large discrepancies observed with the data from Cabañas et al.[24] However, the reasons for the disagreements with the relative rates studies of Zhao et al.[27] and Atkinson et al.[22] can not be explained by this secondary chemistry. To identify the origin of these discrepancies, we have carefully looked for potential sources of artifacts in our experiments. In particular, we have checked that the "low" resolution of our UV−visible spectrometer did not induce an error in the quantification of NO_3. To do that, concentrations obtained with DOASIS software were compared to those obtained by calculating the spectra in absorbance $(\ln(I_0/I))$, integrating the main absorption peak of NO_3 at 662 nm, and deducing the concentration from the Integrated Band Intensity of NO_3. We observed that the concentrations obtained by the two methods were the same within uncertainties.

In conclusion, we did not identify any artifact in our experiments and the reason of the disagreement between our data and those of Zhao et al.[27] and Atkinson et al.[22] remains unclear.

Considering the rate constants obtained in this work, we can deduce that the alkyl chain length of trans-2-alkenals has little or no effect on the rate constants.

Effect of the Structure on the Reactivity. The reaction of NO_3 radicals with unsaturated aldehydes can proceed by two main pathways: an H-atom abstraction from the carbonyl group and an addition to the double bond. It is considered here that the H-abstraction on the alkyl chain is negligible. It is thus interesting to compare the reactivity of the unsaturated carbonyls toward NO_3 radicals with the corresponding alkenes and saturated aldehydes when available (see Table 2) to determine the effect of each group on the reactivity of the other group. For the parent alkenes, no data is available for trans-2-heptene and trans-2-octene. Only rate constants for smaller trans-2-alkenes (trans-2-butene, trans-2-pentene, and trans-2-hexene) have been published. Nevertheless, since no significant trend was observed along the series trans-2-butene, trans-2-pentene, and trans-2-hexene,[32,36] a single rate constant of 3.9×10^{-13} cm^3 molecule^{-1} s^{-1} has been considered for the trans-2-alkenes. By confronting this value with the rate constants for the unsaturated aldehydes, it can be observed that alkenes are much more reactive (by 2 orders of magnitude) than the alkenals. This suggests that the carbonyl group strongly deactivates the addition on the double bond. This could be explained by the electron-withdrawing effect of the carbonyl group in α position.

Moreover, depending on the rate constants, which were chosen for the trans-2-alkenals (this work or previous studies), it can be observed that the rate constants for the unsaturated aldehydes are twice as small or similar to those of the corresponding saturated aldehydes suggesting that the double bond may slightly deactivate the H-abstraction on the carbonyl group. This effect has already been observed by Ullerstam et al.,[26] in their study on the reactivity of crotonaldehyde with NO_3 radicals. Therefore this comparison clearly shows that the association of an aldehyde function and a double bond lowers

Table 2. Comparison of Rate Constants for the Reaction of NO_3 Radical with trans-2-Alkenals Obtained in This Work with Those for the Corresponding Alkenes and Saturated Aldehydes

	compound	k_{NO_3} (cm^3 molecule^{-1} s^{-1})	ref
trans-2-alkenals	trans-2-hexenal	$(4.7 \pm 1.5) \times 10^{-15}$	this work
	trans-2-heptenal	$(5.3 \pm 1.6) \times 10^{-15}$	this work
	trans-2-octenal	$(5.6 \pm 2.3) \times 10^{-15}$	this work
corresponding saturated aldehydes	hexanal	$(1.7 \pm 0.1) \times 10^{-14}$	Noda et al.[44]
		$(1.6 \pm 0.2) \times 10^{-14}$	Noda et al.[44]
		$(1.5 \pm 0.2) \times 10^{-14}$	D'Anna et al.[45]
		$(1.8 \pm 0.4) \times 10^{-14}$	Cabañas et al.[46]
		$(1.5 \pm 0.1) \times 10^{-14}$	Papagni et al.[47]
		$(1.7 \pm 0.2) \times 10^{-14}$	D'Anna et al.[48]
	heptanal	$(1.8 \pm 0.1) \times 10^{-14}$	Noda et al.[44]
		$(1.9 \pm 0.2) \times 10^{-14}$	Noda et al.[44]
		$(2.1 \pm 0.3) \times 10^{-14}$	Noda et al.[44]
		$(2.4 \pm 0.4) \times 10^{-14}$	Cabañas et al.[46]
	octanal	$(1.5 \pm 0.2) \times 10^{-14}$	Noda et al.[44]
		$(2.0 \pm 0.3) \times 10^{-14}$	Noda et al.[44]
corresponding alkenes	trans-2-alkenes	3.9×10^{-13}	Pfrang et al.[36] and IUPAC[32]

the reactivity of both groups. Electronic structure calculations would be helpful to clarify the cause of these deactivating effects.

Product Analysis. Product studies were also carried out for the trans-2-alkenals. An example of the FTIR data for one typical experiment on the reactivity of trans-2-hexenal with NO_3 radical is given in Figure 5. One can observe the quite complex nature of the IR spectra obtained (see spectrum b). However the absorption bands of the trans-2-alkenal between 900 and 1200 cm^{-1} remain identifiable and allow us to quantify it precisely.

The residual spectrum c obtained after subtraction of characteristic bands of reactants, H_2O, N_2O_5, NO_2, and HNO_3, allows the product identification. The absorption band between 2000 and 2200 cm^{-1} indicates the formation of CO. This spectrum also shows several intense absorption bands at around 796 cm^{-1} (NO_2 deformation), 1300 cm^{-1} (NO_2 symmetric stretch), and 1740 cm^{-1} (NO_2 asymmetric stretch), which are characteristic of PAN compounds. Moreover, an absorption band around 1820 cm^{-1} corresponding to C=O stretching modes in peroxyacyl nitrates has also been observed. These absorption bands can be attributed to an unsaturated PAN analogue. This observation is supported by the comparison with Figure 5d, which corresponds to the supposed crotoperoxynitrate (CPAN) spectrum obtained by Orlando et al.,[37] as these two spectra have several similar bands around 1080, 1300, 1740, and 1820 cm^{-1}. In addition, a weak absorption at 845 cm^{-1}, which is characteristic of alkyl nitrates and dinitrates, has been observed in the residual spectra for the experiments on trans-2-heptenal and trans-2-octenal. However, the absorption band was so weak that it could not be quantified. This absorption feature was not observed for trans-2-hexenal. The formation of formic acid is also observed. The origin of this minor product is not known, but may be heterogeneous.

Complementary analyses of carbonyl compounds were performed by sampling the mixtures in impingers containing
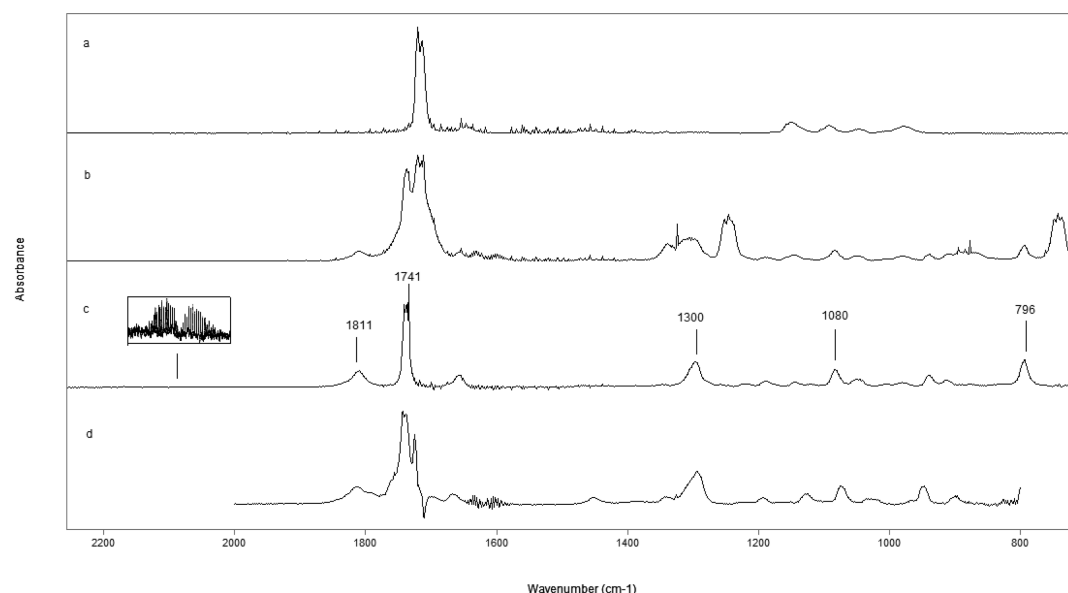
Figure 5. Spectrum (a) is a standard spectrum of *trans*-2-hexenal. Spectrum (b) was obtained after the beginning of the experiment. Spectrum (c) shows a typical product obtained after subtraction of the spectral features belonging to water, *trans*-2-hexenal, N₂O₅, NO₂, and HNO₃. Spectrum (d) corresponds to the presume spectrum of CPAN obtained by Orlando et al.[37]

2,4-dinitrophenylhydrazine solution according to the procedure described by Ferrari et al.[38] The chemical derivatization products were analyzed by high-performance liquid chromatography (HPLC) coupled to UV detection at 360 nm. This technique gives access to a detection limit of ca. 10 ppb for most carbonyls for a sampling volume of 10 L used here. For *trans*-2-hexenal, we did not observe any formation of saturated carbonyl compounds during the course of the experiment. For the *trans*-2-heptenal and *trans*-2-octenal, several peaks have been observed on the chromatograms. Comparison with standards allows us to suspect the formation of acetaldehyde. However, its formation yield could not precisely be calculated and was estimated to be below 3%. Some other peaks which have been detected remain unidentified, but their intensities are very weak suggesting that they might be very minor products.

Despite the fact that no standard spectra of PAN analogues were available, we can estimate their concentration by considering that the IBIs at 796 and 1300 cm⁻¹ of our PAN analogues are equal to those determined by Monedero et al.[39] for the CPAN. Therefore, for the detected products that could be quantified (CO and PAN analogues), yields were derived from initial slopes of plots [product] vs −Δ[*trans*-2-alkenal] and are reported in Table 3. Plots of the concentration of these compounds as a function of *trans*-2-alkenal consumption are given in Supporting Information. The quoted errors take into account the uncertainty in the linear regression (2), the uncertainties in reactant and products IR absorption bands calibration and those in the quantification of these bands in the "mixture" spectra. For comparison, Table 3 also lists the result of mechanistic studies carried out for others α,β-unsaturated aldehydes, i.e., acrolein, methacrolein, and crotonaldehyde.[25,40]

PAN and CO yields for the reaction of NO₃ with the *trans*-2-hexenal are found to be 100 ± 25% and 6.4 ± 4.2%, respectively. The carbon balance is thus complete for this compound. However, it is not the case for the reaction of NO₃ radicals with the *trans*-2-heptenal and *trans*-2-octenal. Indeed for the *trans*-2-heptenal (*trans*-2-octenal), PAN and CO yields are of 64 ± 12% (66 ± 26%) and 5.3 ± 1.8% (4.9 ± 3.3%),

**Table 3. Product Yields Derived from Initial Slopes in the *trans*-2-Alkenals + NO₃ Reactions[a]**

reaction	product	yield (%)	ref
acrolein + NO₃	APAN	47 ± 3	Salgado et al.[25]
	CO	20.9 ± 1.9	
	HCHO	31.6 ± 2.0	
methacrolein + NO₃	MPAN	observed	Canosa-Mas et al.[40]
	CO	observed	
	methylglyoxal	observed	
crotonaldehyde + NO₃	CPAN	93.6 ± 4.3	Salgado et al.[25]
	CO	8.3 ± 1.1	
trans-2-hexenal + NO₃	PAN analogue	100 ± 25	this work
	CO	6.4 ± 4.2	
	formic acid	observed	
trans-2-heptenal + NO₃	PAN analogue	64 ± 12	this work
	CO	5.3 ± 1.8	
	organic nitrates	observed	
	formic acid	observed	
trans-2-octenal + NO₃	PAN analogue	66 ± 26	This work
	CO	4.9 ± 3.3	
	organic nitrates	observed	
	formic acid	observed	

[a]Product yields for acrolein, methacrolein, and crotonaldehyde are included for comparison.

respectively. Thereby for these two compounds, all the products have not been identified. Finally, it can be deduced from this study that PAN-type compounds were the main oxidation products for the three *trans*-2-alkenals. Furthermore, it is interesting to notice that these resulting PAN analogues are stable at room temperature, since no significant decrease in the absorption bands was observed during the experiment but also during a period of one hour after the end of the reaction. Moreover, for some experiments, several ppm of NO were added to the mixture at the end of the reaction in order to promote the decomposition of these PAN, but it has no effect on it (with NO/NO₂ concentration ratios including between 1 and 2).

As mentioned above, the reaction of NO_3 with *trans*-2-alkenals is expected to proceed mainly by both NO_3 addition to the double bond and H-abstraction of the aldehydic hydrogen, the abstraction from the alkyl group being negligible. The formation of a PAN analogue can easily be explained by the abstraction of the aldehydic hydrogen (see channel 3 of Scheme 1). On the contrary, we did not find any mechanism that could

Scheme 1. Proposed Mechanism for the H-Atom Abstraction from the Carbonyl Group on Aliphatic Unsaturated Aldehydes
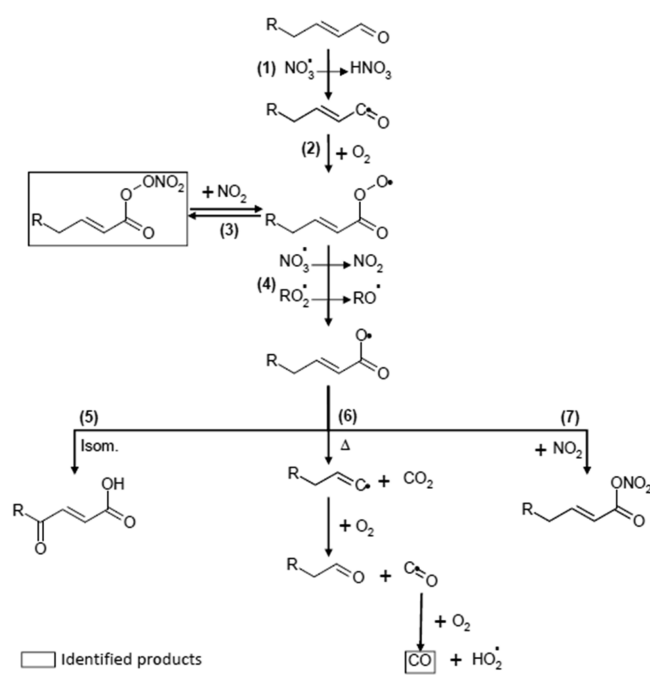
lead to the primary formation of PAN after the addition of NO_3 radicals on the double bond (see the addition mechanism proposed in Figure S8 of the Supporting Information). This suggests that the abstraction of the aldehydic hydrogen is the major reaction pathway for the three unsaturated aldehydes. It should be mentioned that PANs yields obtained here are not necessarily representative of the tropospheric conditions as experiments were carried out with high NO_2 levels (several ppm) whereas tropospheric concentrations do not exceed a few tens of ppb. The consequence is that PANs yields are much higher than those that should be obtained under real tropospheric conditions. However, this does not change the main conclusion of this mechanistic study which is that the H-abstraction is the major pathway. The primary formation of CO may be explained by the scission of the alkoxy radical which results from the reduction of the corresponding peroxy (see channel 6 of Scheme 1). This pathway leads also to the formation of a saturated aldehyde: butanal, pentanal, and hexanal for *trans*-2-hexenal, *trans*-2-heptenal, and *trans*-2-octenal, respectively. However, none of these carbonyl compounds was detected as a primary product by FTIR or by HPLC analyses. Even if we consider a concentration of 10 ppb, which correspond to the detection limit of these compounds, their yields would be of 0.5%. Thereby, their yields would be much lower than CO yields, which mean that they cannot be coproducts. Therefore, CO obtained is not

formed by the channel 6 and could probably result from the addition channel.

From these results, the branching ratio of the abstraction pathway can be estimated as follow: 1 ± 0.25 for *trans*-2-hexenal > 0.64 for *trans*-2-heptenal and >0.66 for *trans*-2-octenal. The observations made here are similar to the one made by Salgado et al.[25] in their study on the reactivity of crotonaldehyde and acrolein with NO_3 radicals. Indeed these latter authors mainly detect the formation of products resulting from the abstraction channel (see Table 3) and in particular APAN and CPAN. Canosa-Mas et al.[40] have studied the reactivity of methacrolein with NO_3 radicals. Even if the authors could not provide formation yields, they also observed that MPAN (methacryloylperoxynitrate) is a major product. These conclusions are quite unexpected considering the significant reactivity of the substituted double bonds compared to the −CHO function. Indeed, according to Table 2, *trans*-2-alkenes are up to 20 times more reactive than saturated aldehydes. Thereby all these studies confirm the strong deactivating effect of the aldehydic group on the double bond since the main reaction pathway is the abstraction of the aldehydic hydrogen. Notwithstanding, to confirm and explain these observations further chamber experiments (including the study of the kinetic isotope effect) and computational studies would be useful.

■ CONCLUSIONS AND ATMOSPHERIC IMPLICATIONS

Rate constants for three unsaturated aldehydes have been measured using an absolute rate method. The rate constants obtained in this study led to a significant re-evaluation of previously published values. The rate constants measured here for the *trans*-2-hexenal and *trans*-2-heptenal are in particular much lower than those obtained by Cabañas et al.[24] using absolute rate technique and to a lesser extent to those by relative rate technique.[22,27]

Thereby, our study reveals that the alkyl chain of the *trans*-2-alkenals has no significant effect on their reactivity with the nitrate radical. The aldehydic function appears to decrease the reactivity of the neighboring double bond, and unexpectedly, a double bond appears also to lower the reactivity of the aldehydic hydrogen atom. Thus, this work provides crucial information for the extension to the aldehydes of the SAR developed recently in our group.[28]

Furthermore the mechanisms of the reactions between the nitrate radical and the three *trans*-2-alkenals have been studied, and the PAN-type compounds have been identified as major products. Therefore this work indicates that the abstraction of the aldehydic hydrogen is the dominant pathway at room temperature for the NO_3 radical reactions with these three unsaturated carbonyl compounds.

The typical tropospheric lifetimes of the *trans*-2-alkenals have been estimated using the rate coefficients determined in this study and the rate constants for their reactions with OH and O_3 obtained from literature. Typical tropospheric concentrations were used for the oxidants: 1.6×10^6 molecules cm^{-3} for OH radicals,[41] 5×10^8 molecules cm^{-3} for NO_3 radicals,[42] and 7×10^{11} molecules cm^{-3} for ozone.[43] These lifetimes are given in Table 4. It can clearly be seen that tropospheric lifetimes toward OH radicals, being on the order of a few hours, are significantly shorter than those estimated with respect to the NO_3 and ozone reactions which have been found to be around few days. Therefore, the daytime OH-oxidation is the dominant

Table 4. Calculated Tropospheric Lifetimes of *trans*-2-Hexenal, *trans*-2-Heptenal, and *trans*-2-Octenal from Gas-Phase Reactions with OH Radicals, NO$_3$ Radicals, and O$_3$

compound	τ_{OH}	τ_{NO_3}	τ_{O_3}
trans-2-hexenal	3.9 h[49]	5.0 day this work	8 day[22]
trans-2-heptenal	3.9 h[49]	4.4 day this work	
trans-2-octenal	4.3 h[50]	4.2 day this work	

chemical removal pathway for these unsaturated aldehydes in the troposphere.

■ ASSOCIATED CONTENT

Ⓢ Supporting Information
Experimental plots of concentrations of reactants, nitrogen species (*trans*-2-hexenal, NO$_2$, PAN analogue), and CO measured by FTIR and by UV–visible absorption spectrometry (NO$_3$) vs time (Figure S1), formation yields of the PAN analogue during NO$_3$ oxidation of *trans*-2-hexenal (Figure S2), formation yields of CO during NO$_3$ oxidation of *trans*-2-hexenal (Figure S3), formation yields of PAN analogue during NO$_3$ oxidation of *trans*-2-heptenal (Figure S4), formation yields of CO during NO$_3$ oxidation of *trans*-2-octenal (Figure S5), formation yields of PAN analogue during NO$_3$ oxidation of *trans*-2-octenal (Figure S6), formation yields of CO during NO$_3$ oxidation of *trans*-2-octenal (Figure S7), proposed mechanism for the NO$_3$ radical addition to the double bond on aliphatic unsaturated aldehydes (Figure S8). This material is available free of charge via the Internet at http://pubs.acs.org.

■ AUTHOR INFORMATION

Corresponding Author
*Fax: +33 1451 71564. Phone: +33 1451 71586. E-mail: picquet@lisa.u-pec.fr.

Notes
The authors declare no competing financial interest.

■ ACKNOWLEDGMENTS

■ REFERENCES

(1) Graedel, T. E. *Chemical Compounds in the Atmosphere*; Academic Press: New York, 1978.
(2) Grosjean, D.; Grosjean, E.; Gertler, A. W. *Environ. Sci. Technol.* **2000**, *35*, 45−53.
(3) Kean, A. J.; Grosjean, E.; Grosjean, D.; Harley, R. A. *Environ. Sci. Technol.* **2001**, *35*, 4198−4204.
(4) Carlier, P.; Hannachi, H.; Mouvier, G. *Atmos. Environ.* **1986**, *20*, 2079−2099.
(5) Guenther, A.; Geron, C.; Pierce, T.; Lamb, B.; Harley, P.; Fall, R. *Atmos. Environ.* **2000**, *34*, 2205−2230.
(6) Wildt, J.; Kobel, K.; Schuh-Thomas, G.; Heiden, A. C. *J. Atmos. Chem.* **2003**, *45*, 173−196.
(7) Arey, J.; Winer, A. M.; Atkinson, R.; Aschmann, S. M.; Long, W. D.; Lynn Morrison, C. *Atmos. Environ.* **1991**, *25*, 1063−1075.
(8) Kirstine, W.; Galbally, I.; Ye, Y.; Hooper, M. *J. Geophys. Res.* **1998**, *103*, 10605−10619.
(9) Fall, R.; Karl, T.; Hansel, A.; Jordan, A.; Lindinger, W. *J. Geophys. Res.* **1999**, *104*, 15963−15974.
(10) Springett, M. B.; Williams, B. M.; Barnes, R. J. *Food Chem.* **1994**, *49*, 393−398.
(11) Boué, S. M.; Shih, B. Y.; Carter-Wientjes, C. H.; Cleveland, T. E. *J. Agric. Food Chem.* **2003**, *51*, 4873−4876.
(12) Sinyinda, S.; Gramshaw, J. W. *Food Chem.* **1998**, *62*, 483−487.
(13) Cramer, A.-C. J.; Mattinson, D. S.; Fellman, J. K.; Baik, B.-K. *J. Agric. Food Chem.* **2005**, *53*, 7526−7531.
(14) Calogirou, A.; Larsen, B. R.; Kotzias, D. *Atmos. Environ.* **1999**, *33*, 1423−1439.
(15) Jemma, C. A.; Shore, P. R.; Widdicombe, K. A. *J. Chromatogr. Sci.* **1995**, *33*, 34−48.
(16) Finlayson-Pitts, B. J.; Pitts Jr., J. N. *Chemistry of the Upper and Lower Atmosphere*; Academic Press: San Diego, 2000.
(17) Mellouki, A.; Le Bras, G.; Sidebottom, H. *Chem. Rev.* **2003**, *103*, 5077−5096.
(18) Kanakidou, M.; Seinfeld, J. H.; Pandis, S. N.; Barnes, I.; Dentener, F. J.; Facchini, M. C.; Van Dingenen, R.; Ervens, B.; Nenes, A.; Nielsen, C. J.; Swietlicki, E.; Putaud, J. P.; Balkanski, Y.; Fuzzi, S.; Horth, J.; Moortgat, G. K.; Winterhalter, R.; Myhre, C. E. L.; Tsigaridis, K.; Vignati, E.; Stephanou, E. G.; Wilson, J. *Atmos. Chem. Phys.* **2005**, *5*, 1053−1123.
(19) Atkinson, R. *Atmos. Environ.* **2007**, *41*, 200−240.
(20) Wayne, R. P.; Barnes, I.; Biggs, P.; Burrows, J. P.; Canosa-Mas, C. E.; Hjorth, J.; Le Bras, G.; Moortgat, G. K.; Perner, D.; Poulet, G.; Restelli, G.; Sidebottom, H. *Atmos. Environ.* **1991**, *25*, 1−203.
(21) Atkinson, R. *J. Phys. Chem. Ref. Data* **1991**, *20*, 459−507.
(22) Atkinson, R.; Arey, J.; Aschmann, S. M.; Corchnoy, S. B.; Shu, Y. *Int. J. Chem. Kinet.* **1995**, *27*, 941−955.
(23) Atkinson, R.; Aschmann, S. M.; Goodman, M. A. *Int. J. Chem. Kinet.* **1987**, *19*, 299−307.
(24) Cabanas, B.; Salgado, S.; Martin, P.; Baeza, M. T.; Martinez, E. *J. Phys. Chem. A* **2001**, *105*, 4440−4445.
(25) Salgado, M. S.; Monedero, E.; Villanueva, F.; Martin, P.; Tapia, A.; Cabanas, B. *Environ. Sci. Technol.* **2008**, *42*, 2394−2400.
(26) Ullerstam, M.; Ljungström, E.; Langer, S. *Phys. Chem. Chem. Phys.* **2001**, *3*, 986−992.
(27) Zhao, Z. J.; Husainy, S.; Smith, G. D. *J. Phys. Chem. A* **2011**, *115*, 12161−12172.
(28) Kerdouci, J.; Picquet-Varrault, B.; Doussin, J. F. *ChemPhysChem* **2010**, *11*, 3909−3920.
(29) Doussin, J. F.; Ritz, D.; Durand-Jolibois, R.; Monod, A.; Carlier, P. *Analusis* **1997**, *25*, 236−242.
(30) Picquet-Varrault, B.; Orphal, J.; Doussin, J. F.; Carlier, P.; Flaud, J. M. *J. Phys. Chem. A* **2005**, *109*, 1008−1014.
(31) Atkinson, R.; Plum, C. N.; Carter, W. P. L.; Winer, A. M.; Pitts, J. N. *J. Phys. Chem.* **1984**, *88*, 1210−1215.
(32) IUPAC. Subcommittee on Gas Kinetic Data Evaluation, Evaluated Kinetic Data, http://www.iupac-kinetic.ch.cam.ac.uk/.
(33) Brauers, T.; Finlayson-Pitts, B., J. *Int. J. Chem. Kinet.* **1997**, *29*, 665−672.
(34) Ullerstam, M.; Langer, S.; Ljungström, E. *Int. J. Chem. Kinet.* **2000**, *32*, 294−303.
(35) D'Anna, B.; Langer, S.; Ljungstrom, E.; Nielsen, C. J.; Ullerstam, M. *Phys. Chem. Chem. Phys.* **2001**, *3*, 1631−1637.
(36) Pfrang, C.; Martin, R. S.; Nalty, A.; Waring, R.; Canosa-Mas, C. E.; Wayne, R. P. *Phys. Chem. Chem. Phys.* **2005**, *7*, 2506−2512.
(37) Orlando, J. J.; Tyndall, G. S. *J. Phys. Chem. A* **2002**, *106*, 12252−12259.

10141

dx.doi.org/10.1021/jp3071234 | *J. Phys. Chem. A* 2012, 116, 10135−10142

(38) Ferrari, C. P.; Durand-Jolibois, R.; Carlier, P.; Jacob, V.; Roche, A.; Foster, P.; Fresnet, P. *Analusis* **1999**, *27*, 45−53.

(39) Monedero, E.; Salgado, M. S.; Villanueva, F.; Martin, P.; Barnes, I.; Cabanas, B. *Chem. Phys. Lett.* **2008**, *465*, 207−211.

(40) Canosa-Mas, C. E.; Carr, S.; King, M. D.; Shallcross, D. E.; Thompson, K. C.; Wayne, R. P. *Phys. Chem. Chem. Phys.* **1999**, *1*, 4195−4202.

(41) Prinn, R. G.; Weiss, R. F.; Miller, B. R.; Huang, J.; Alyea, F. N.; Cunnold, D. M.; Fraser, P. J.; Hartley, D. E.; Simmonds, P. G. *Science* **1995**, *269*, 187−192.

(42) Shu, Y.; Atkinson, R. *J. Geophys. Res.* **1995**, *100*, 7275−7281.

(43) Logan, J. A. *J. Geophys. Res.* **1985**, *90*, 10463−10482.

(44) Noda, J.; Holm, C.; Nyman, G.; Langer, S.; Ljungström, E. *Int. J. Chem. Kinet.* **2003**, *35*, 120−129.

(45) D'Anna, B.; Andresen, O.; Gefen, Z.; Nielsen, C. J. *Phys. Chem. Chem. Phys.* **2001**, *3*, 3057−3063.

(46) Cabanas, B.; Martin, P.; Salgado, S.; Ballesteros, B.; Martinez, E. *J. Atmos. Chem.* **2001**, *40*, 23−39.

(47) Papagni, C.; Arey, J.; Atkinson, R. *Int. J. Chem. Kinet.* **2000**, *32*, 79−84.

(48) D'Anna, B.; Nielsen, C. J. *J. Chem. Soc., Faraday Trans.* **1997**, *93*, 3479−3483.

(49) Davis, M. E.; Gilles, M. K.; Ravishankara, A. R.; Burkholder, J. B. *Phys. Chem. Chem. Phys.* **2007**, *9*, 2240−2248.

(50) Gao, T.; Andino, J. M.; Rivera, C. C.; Marquez, M. F. *Int. J. Chem. Kinet.* **2009**, *41*, 483−489.